

Electron correlation in the two-dimensional triangle lattice of Na_xCoO_2

J. Sugiyama^{1,*}, J. H. Brewer², E. J. Ansaldo³, B. Hitti³, M. Mikami^{4,†}, Y. Mori⁴, and T. Sasaki⁴

¹*Toyota Central Research and Development Labs. Inc., Nagakute, Aichi 480-1192, Japan*

²*TRIUMF, CIAR and Department of Physics and Astronomy,*

University of British Columbia, Vancouver, BC, V6T 1Z1 Canada

³*TRIUMF, 4004 Wesbrook Mall, Vancouver, BC, V6T 2A3 Canada and*

⁴*Department of Electrical Engineering, Osaka University, Suita, Osaka 563-8577, Japan*

(Dated: November 5, 2018)

Magnetism of layered cobaltites Na_xCoO_2 with $x = 0.6$ and 0.9 has been investigated by a positive muon spin rotation and relaxation ($\mu^+\text{SR}$) spectroscopy together with magnetic susceptibility and specific heat measurements, using single crystal samples in the temperature range between 250 and 1.8 K. Zero-field (ZF-) $\mu^+\text{SR}$ measurements on $\text{Na}_{0.9}\text{CoO}_2$ indicates a transition from a paramagnetic to an incommensurate spin density wave state at 19 K ($=T_{\text{SDW}}$). The anisotropic ZF- $\mu^+\text{SR}$ spectra suggest that the oscillating moments of the IC-SDW directs along the c -axis. Since $\text{Na}_{0.6}\text{CoO}_2$ is paramagnetic down to 1.8 K, the magnitude of T_{SDW} is found to strongly depend on x . This behavior is well explained using the Hubbard model within a mean field approximation on two-dimensional triangle lattice in the CoO_2 plane. Also, both the appearance of the IC-SDW state by the change in x and the magnitude of the electronic specific heat parameter of $\text{Na}_{0.6}\text{CoO}_2$ indicate that Na_xCoO_2 is unlikely to be a typical strongly correlated electron system.

PACS numbers: 76.75.+i, 75.30.Fv, 72.15.Jf, 65.40.Ba

I. INTRODUCTION

Layered cobaltites with a two-dimensional-triangular lattice (2DTL) of Co ions have been intensely investigated because of their structural variety, promising thermoelectric performance, [1, 2, 3, 4, 5, 6, 7, 8] and unpredictable superconducting behavior induced by an intercalation of H_2O . [9, 10, 11] Among them, the sodium cobaltite Na_xCoO_2 is apparently the most basic compound, because of its simple structure, the single CoO_2 planes and the single disordered Na planes form alternating stacks along the c axis. [12] The CoO_2 planes, in which the 2DTL of Co ions is formed by a network of edge-sharing CoO_6 octahedra, are the conduction planes of Na_xCoO_2 . Therefore, the magnetic and transport properties of Na_xCoO_2 are expected to strongly depend on the nominal valence of the Co ions in the CoO_2 planes, similar to the case of the CuO_2 planes for the high- T_c cuprates.

Motohashiet *al.* reported the existence of a magnetic transition at 22 K ($= T_m$) in polycrystalline $\text{Na}_{0.75}\text{CoO}_2$ from the observation of small changes in bulk susceptibility and transport properties, while no transitions were found in $\text{Na}_{0.65}\text{CoO}_2$ down to 2 K. [14] Recent positive muon spin rotation and relaxation ($\mu^+\text{SR}$) experiment on a polycrystalline $\text{Na}_{0.75}\text{CoO}_2$ sample [15] indicated that the transition at 22 K is not induced by impurities but is an intrinsic change in the magnetism of the sample,

although the sample was magnetically inhomogeneous. Furthermore, the $\mu^+\text{SR}$ result suggested that the ordered phase below T_m could be either a ferrimagnetic (FR) or a commensurate (C) spin density wave (SDW) state. [15]

On the other hand, the related compound, pure and doped $[\text{Ca}_2\text{CoO}_3]_{0.62}^{\text{RS}}[\text{CoO}_2]$ (RS denotes the rocksalt-type subsystem), exhibited a transition to an incommensurate (IC) SDW state below ~ 100 K. [16] Recent $\mu^+\text{SR}$ experiment using both single crystals and c -aligned polycrystals suggested that long-range IC-SDW order forms below ~ 30 K ($\equiv T_{\text{SDW}}$), while a short-range order appears below 100 K ($\equiv T_c^{\text{on}}$). [17, 18] Also, the IC-SDW was found to be induced by the ordering of the Co spins in the CoO_2 planes.

The magnetically ordered state is, therefore, most likely common for the 2DTL of the Co ions in the layered cobaltites. The relationship between the transition temperature and the Co valence is, therefore, worth to investigate in order to better understand the nature of the 2DTL. In particular, the Co valence in the CoO_2 planes changes directly in proportion to x for Na_xCoO_2 , whereas that is unclear for $[\text{Ca}_2\text{CoO}_3]_{0.62}^{\text{RS}}[\text{CoO}_2]$ because of the two nonequivalent Co sites in the lattice. It should be noted that the polycrystalline $\text{Na}_{0.75}\text{CoO}_2$ sample, although structurally single phase, was found to be magnetically inhomogeneous. [15] Hence, the $\mu^+\text{SR}$ experiments on single crystals are important for further elucidation of the nature of the 2DTL.

The detailed crystal structure of Na_xCoO_2 was reported to depend on x and reaction temperature; [12] that is, α - Na_xCoO_2 with $0.9 \leq x \leq 1$, α' - Na_xCoO_2 with $x=0.75$, β - Na_xCoO_2 with $0.55 \leq x \leq 0.6$ and γ - Na_xCoO_2 with $0.55 \leq x \leq 0.74$. Also, the structure of $\text{Na}_{0.5}\text{CoO}_2$ was reported to be assigned as the γ -phase. [13] Un-

*Electronic address: e0589@mosk.tytlabs.co.jp

†Present address: National Institute of Advanced Industrial Science and technology, Ikeda, Osaka 563-8577, Japan.

fortunately, single crystals are available only for the α - Na_xCoO_2 phase with $x=0.9$ and the γ - Na_xCoO_2 phase with $x=0.6$,[19] and attempts to prepare crystals with the other x have failed so far. Magnetic susceptibility (χ) measurements on these crystals indicated that α - $\text{Na}_{0.9}\text{CoO}_2$ exhibits a magnetic transition at ~ 20 K, whereas γ - $\text{Na}_{0.6}\text{CoO}_2$ seems to be a Curie-Weiss paramagnet down to 5 K.[20] Also, the resistivity (ρ)-vs- T curve in α - $\text{Na}_{0.9}\text{CoO}_2$ was found to be metallic above ~ 20 K, while semiconducting below ~ 20 K.[19, 20]

We report both weak (65 Oe) transverse-field (wTF-) μ^+ SR and zero field (ZF-) μ^+ SR measurements for single crystal platelets of $\text{Na}_{0.9}\text{CoO}_2$ and $\text{Na}_{0.6}\text{CoO}_2$ at temperatures below 300 K to further elucidate the relationship between the transition temperature and the Co valence, *i.e.*, the magnetic phase diagram. In addition, we performed heat capacity measurements on these crystals to study the magnetism of Na_xCoO_2 in full detail.

II. EXPERIMENTAL

Single crystals of Na_xCoO_2 were grown at Osaka University by a flux technique using reagent grade Na_2CO_3 and Co_3O_4 powders as starting materials. A mixture of NaCl , Na_2CO_3 and B_2O_3 was used as the flux. The typical dimension of the obtained $\text{Na}_{0.9}\text{CoO}_2$ platelets was $\sim 3 \times 3 \times 0.1$ mm³, while that of $\text{Na}_{0.6}\text{CoO}_2$ was $\sim 6 \times 6 \times 0.1$ mm³. The preparation and characterization of these crystals were reported in greater detail elsewhere.[19, 20]

Susceptibility (χ) was measured using a superconducting quantum interference device (SQUID) magnetometer (mpms, Quantum Design) in the temperature range between 400 and 5 K under magnetic field $H \leq 55$ kOe. In order to increase the magnetic signal, 5 platelets were stacked in a plastic sample holder. Also, to determine anisotropy, H was applied parallel or perpendicular to the basal (*i.e.*, c) plane. Hereby, we will abbreviate susceptibility obtained with $H//c$ as χ_c and $H \perp c$ as χ_a , respectively.

Heat capacity (C_p) was measured using a relaxation technique (ppms, Quantum Design) in the temperature range between 300 and 1.9 K. The μ^+ SR experiments were performed on the M20 and M15 surface muon beam lines at TRIUMF. The experimental setup and techniques were described elsewhere.[21]

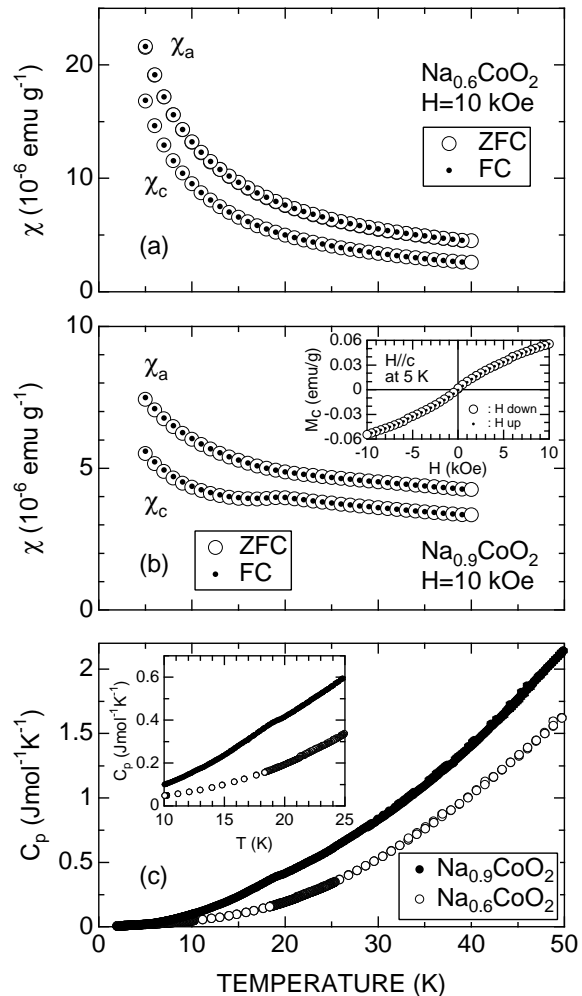


FIG. 1: (a) Temperature dependences of magnetic susceptibility χ for $\text{Na}_{0.6}\text{CoO}_2$ and (b) $\text{Na}_{0.9}\text{CoO}_2$ and (c) temperature dependence of heat capacity C_p for $\text{Na}_{0.9}\text{CoO}_2$ and $\text{Na}_{0.6}\text{CoO}_2$. The inset in Fig. 1(b) shows the magnetization M as a function of magnetic field H at 5 K and that in Fig. 1(c) the magnification of the $C_p(T)$ curve in the vicinity of T_c . χ was measured both in zero field-cooling ZFC and field-cooling FC mode with $H = 10$ kOe and H applied parallel and perpendicular to the c axis.

III. RESULTS

A. susceptibility and heat capacity

The temperature dependence of χ_c for the $\text{Na}_{0.9}\text{CoO}_2$ crystal exhibits a clear cusp at 19 K ($=T_c$), whereas no clear anomalies in the $\chi_a(T)$ curve (see Fig. 1(b)). Since there is no marked difference between the data obtained in zero field cooling (ZFC) and field cooling (FC) mode, this cusp is most likely due to an antiferromagnetic transition. Actually, the relationship between magnetization

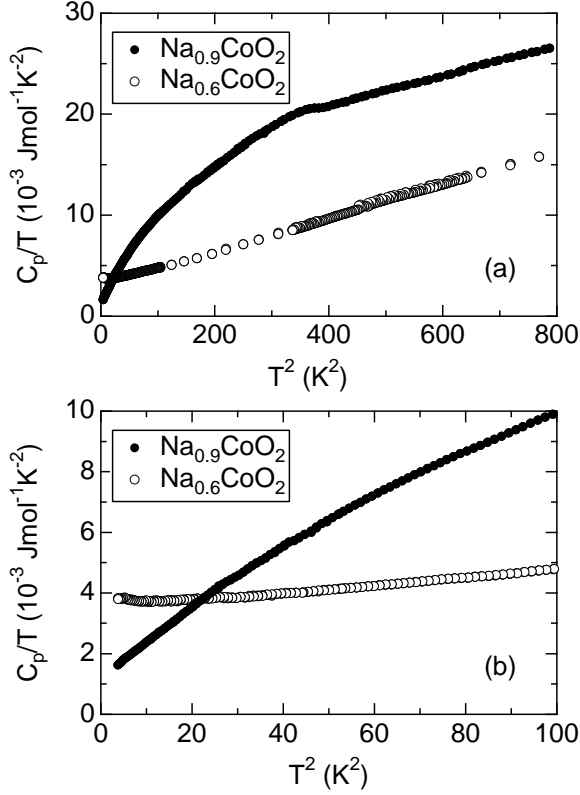


FIG. 2: (a) The relationship between C_p/T and T^2 for $\text{Na}_{0.9}\text{CoO}_2$ and $\text{Na}_{0.6}\text{CoO}_2$; (a) $0 \leq T^2 \leq 800 \text{ K}^2$ and (b) $0 \leq T^2 \leq 100 \text{ K}^2$

M_c and H has no loop even at 5 K (see the inset of Fig. 1(b)) The $\chi(T)$ curves for the $\text{Na}_{0.6}\text{CoO}_2$ crystal show a paramagnetic behavior down to 5 K with a small anisotropy, as reported.[20]

The $C_p(T)$ curve for the $\text{Na}_{0.9}\text{CoO}_2$ crystal also exhibits a small maximum at 19 K, indicating the transition detected by the χ measurement. On the other hand, C_p for the $\text{Na}_{0.6}\text{CoO}_2$ crystal decreases monotonically with decreasing T down to 1.9 K. Note that in Fig. 1(c) 1 mol denotes 1 mol atom; thus, C_p for Na_xCoO_2 is equivalent to the measured heat capacity ($\text{Jg}^{-1}\text{K}^{-1}$) divided by $(3+x)M$, where M is the molar weight of Na_xCoO_2 . The dependence of C_p/T on T^2 for $\text{Na}_{0.9}\text{CoO}_2$ looks very complicated due to a contribution of the magnetic order, although the C_p/T -vs- T^2 curve for $\text{Na}_{0.6}\text{CoO}_2$ exhibits an almost linear relation in the T^2 range above 30 K^2 (see Fig. 2). This is also evidence for lack of magnetic order in $\text{Na}_{0.6}\text{CoO}_2$ down to 1.9 K.

If we employ the Debye formula

$$\frac{C_p}{T} = \gamma + \beta T^2, \quad (1)$$

in the T^2 range between 30 and 100 K^2 , we obtain the electronic specific heat parameter $\gamma = 3.62 \pm 0.04 \text{ mJK}^{-2}$

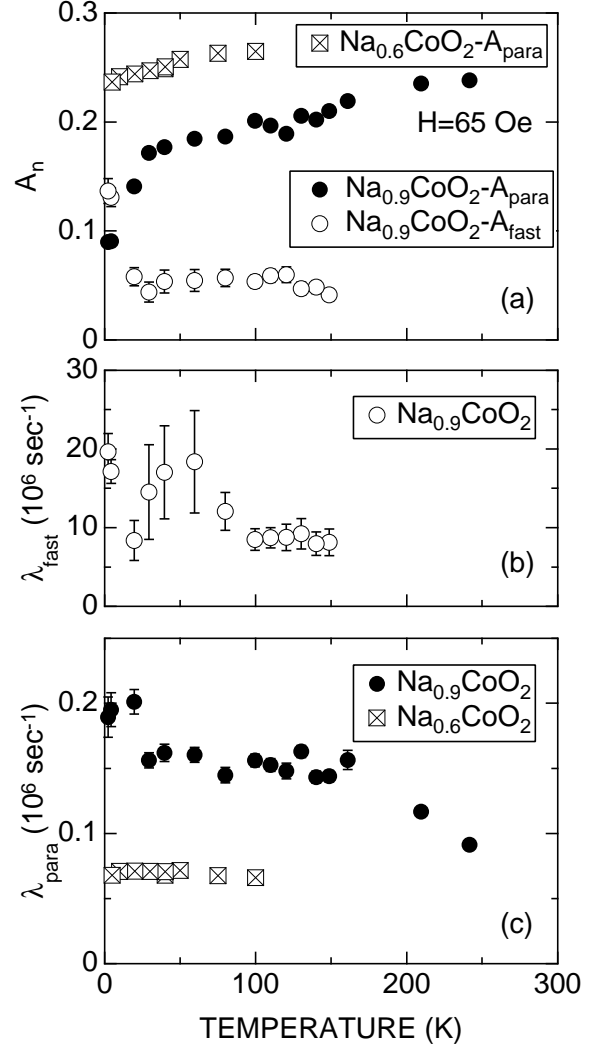


FIG. 3: Temperature dependences of (a) A_{para} and A_{fast} , (b) λ_{fast} and (c) λ_{para} in single crystal platelets of $\text{Na}_{0.9}\text{CoO}_2$ (solid and open circles) and $\text{Na}_{0.6}\text{CoO}_2$ (crossed squares). The data were obtained by fitting the wTF- μ^+ SR spectra with Eq. (2).

per mol atom and $\beta = 0.0614 \pm 0.0004 \text{ mJmolK}^{-4}$ per mol atom. This gives the Debye temperature (θ_D) of 316 K. Two different platelets of $\text{Na}_{0.6}\text{CoO}_2$ provided almost same values of γ and θ_D . Making comparison with the data for the polycrystalline $\text{Na}_{0.55}\text{CoO}_2$ ($\gamma = 6.8 \text{ mJK}^{-2}$ per mol atom and $\theta_D = 354 \text{ K}$),[22] the present values are rather small, probably due to the effects of grain boundaries and/or undetected second phases in the polycrystals. Furthermore, the present γ is in good agreement with the value calculated for band structure of $\text{Na}_{0.5}\text{CoO}_2$ ($\gamma = 3 \text{ mJK}^{-2}$ per mol atom).[23]

B. wTF- μ^+ SR

The wTF- μ^+ SR spectra in a magnetic field of $H \sim 65$ Oe in the $\text{Na}_{0.9}\text{CoO}_2$ crystals exhibit a clear reduction of the μ^+ precession paramagnetic amplitude below T_c . The wTF- μ^+ SR spectrum below T_c was well fitted in the time domain with a combination of a slowly relaxing precessing signal and a fast non-oscillatory signal, as in the case of $[\text{Ca}_2\text{CoO}_3]_{0.62}^{\text{RS}}[\text{CoO}_2]$: [16]

$$A_0 P(t) = A_{\text{para}} \exp(-\lambda_{\text{para}} t) \cos(\omega_{\mu} t + \phi) + A_{\text{fast}} \exp(-\lambda_{\text{fast}} t), \quad (2)$$

where A_0 is the initial asymmetry, $P(t)$ is the muon spin polarization function, ω_{μ} is the muon Larmor frequency, ϕ is the initial phase of the precession and A_n and λ_n ($n = \text{para}$ and fast) are the asymmetries and exponential relaxation rates of the two signals. Interestingly, the non-oscillatory signal ($n = \text{fast}$) has finite amplitudes below ~ 150 K.

Figures 3(a) - 3(c) show the temperature dependences of A_n and λ_n ($n = \text{para}$ and fast) in $\text{Na}_{0.9}\text{CoO}_2$ and $\text{Na}_{0.6}\text{CoO}_2$. For $\text{Na}_{0.9}\text{CoO}_2$, as T decreases from 250 K, the magnitude of A_{para} decreases monotonically down to T_c , then slope (dA_{para}/dT) suddenly steepens with further lowering T . Also, the $A_{\text{fast}}(T)$ curve is nearly constant down to T_c and then suddenly increases with T . On the other hand, as T decreases from 250 K, $\lambda_{\text{para}}(T)$ increases down to 150 K, roughly levels off to a constant value down to T_c , and then suddenly increases at T_c and again levels off to a constant value below T_c . Considering the large experimental error, the $\lambda_{\text{fast}}(T)$ curve is approximately a constant down to T_c and then suddenly increases with T .

These behaviors clearly indicate the existence of a transition to a magnetically ordered state at T_c in $\text{Na}_{0.9}\text{CoO}_2$, as expected by the χ and C_p measurements. Furthermore, the μ^+ SR data show other changes at around 150 K. The transport measurements (resistivity ρ and Seebeck coefficient S), both the $d\rho/dT(T)$ and $S(T)$ curves exhibited a broad maximum around 150 K, whereas no clear anomalies were seen in the $\chi(T)$ curve. [19, 20]

Furthermore, there are no marked changes in both $A_{\text{para}}(T)$ and $\lambda_{\text{para}}(T)$ in $\text{Na}_{0.6}\text{CoO}_2$. This indicates that the Na-poorer crystal is a paramagnet down to 5 K, consistent with the results of the χ and C_p measurements.

C. ZF- μ^+ SR

Figure 4(a) shows ZF- μ^+ SR time spectrum at 1.8 K in the single crystal platelets of $\text{Na}_{0.9}\text{CoO}_2$; the spectrum was obtained with the initial μ^+ spin direction $\vec{S}_{\mu}(0)$ perpendicular to the c -axis. A clear oscillation due to quasi-static internal fields is observed only when $\vec{S}_{\mu}(0) \perp \hat{c}$.

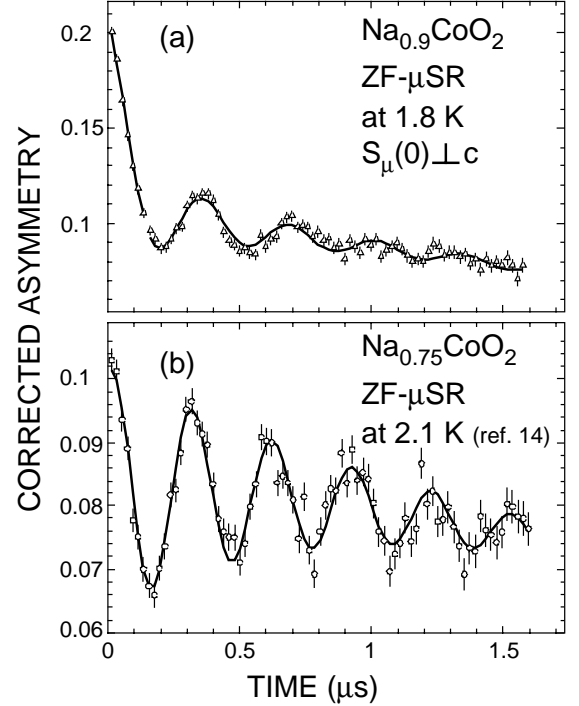


FIG. 4: ZF- μ^+ SR time spectra of (a) single crystal platelets of $\text{Na}_{0.9}\text{CoO}_2$ at 1.8 K and (b) a polycrystalline plate of $\text{Na}_{0.75}\text{CoO}_2$ at 2.1 K (ref. 14). In Fig. 4(a), the configuration of the sample and the initial muon spin direction $\vec{S}_{\mu}(0)$ is $\vec{S}_{\mu}(0) \perp \hat{c}$. Both a rapid initial decay of the amplitude and a delay of the initial phase in the top spectrum indicate that an incommensurate spin structure presents in $\text{Na}_{0.9}\text{CoO}_2$, whereas a commensurate structure in $\text{Na}_{0.75}\text{CoO}_2$.

Also, the ZF- μ^+ SR time spectrum for the polycrystalline $\text{Na}_{0.75}\text{CoO}_2$ sample, which entered a commensurate spin structure below 22 K, [15] is shown in Fig. 4(b). Making comparison with the bottom spectrum, the oscillation amplitude in the top spectrum decays rapidly and the initial phase delays. The oscillation in the top spectrum is characteristic of a zeroth-order Bessel function of the first kind $J_0(\omega_{\mu} t)$ that describes the muon polarization evolution in an IC-SDW field distribution. [24, 25] Actually, the top oscillating spectrum was fitted using a combination of three signals:

$$A_0 P(t) = A_{\text{SDW}} J_0(\omega_{\mu} t) \exp(-\lambda_{\text{SDW}} t)^{\beta_{\text{SDW}}} + A_{\text{KT}} G_{zz}^{\text{KT}}(t, \Delta) + A_x \exp(-\lambda_x t)^{\beta_x}, \quad (3)$$

$$\omega_{\mu} \equiv 2\pi\nu_{\mu} = \gamma_{\mu} H_{\text{int}}, \quad (4)$$

$$G_{zz}^{\text{KT}}(t, \Delta) = \frac{1}{3} + \frac{2}{3} (1 - \Delta^2 t^2) \exp(-\frac{\Delta^2 t^2}{2}), \quad (5)$$

where A_0 is the empirical maximum muon decay asymmetry, A_{SDW} , A_{KT} and A_x are the asymmetries associated with the three signals, $G_{zz}^{\text{KT}}(t, \Delta)$ is the static Gaussian Kubo-Toyabe function, Δ is the static width of the distribution of local frequencies at the disordered sites, λ_x is the slow relaxation rate and β_{SDW} and β_x are the power of the exponential relaxation. Fits using just an exponentially damped cosine oscillation, $\exp(-\lambda t) \cos(\omega_\mu t + \phi)$, provides a phase angle $\phi \sim -42^\circ$, which is physically meaningless,[26] although $\phi \sim 0^\circ$ for the bottom spectrum. [15]

We therefore conclude that $\text{Na}_{0.9}\text{CoO}_2$ undergoes a magnetic transition from a paramagnetic state to an IC-SDW state (*i.e.* $T_c = T_{\text{SDW}}$). The absence of a clear oscillation in the spectrum obtained with $\vec{S}_\mu(0) \parallel \hat{c}$ indicates that the internal magnetic field \vec{H}_{int} is roughly parallel to the c -axis, since the muon spins do not precess in a parallel magnetic field. The IC-SDW is unlikely to propagate along the c -axis due to the two-dimensionality. The IC-SDW is therefore concluded to propagate in the c plane (*i.e.*, the $[\text{CoO}_2]$ plane), with oscillating moments directed along the c -axis, as in the case of $[\text{Ca}_2\text{CoO}_3]_{0.62}^{\text{RS}}[\text{CoO}_2]$. [18] Moreover, this anisotropic result is consistent with χ measurements. That is, the cusp at 19 K was observed, when H was applied parallel to the c axis, whereas the cusp was undetected if $H \perp c$. [20]

Figures 5(a)-5(e) show the temperature dependences of (a) A_{SDW} , A_{KT} and A_x , (b) the volume fraction of the SDW signal (V_{F}), (c) λ_{SDW} , Δ and λ_x and (d) β_{SDW} and β_x (e) ν_μ for the single crystal platelets of $\text{Na}_{0.9}\text{CoO}_2$. The volume fraction (V_{F}) was calculated as $A_{\text{SDW}}/(A_{\text{SDW}} + A_{\text{KT}} + A_x)$. The magnitude of A_{SDW} increases with decreasing T below T_{SDW} , although both A_{KT} and A_x are almost T independent. (see Fig. 5(a)). Here, the static Gaussian Kubo-Toyabe function is for the signal from muon sites experiencing disordered magnetic fields, and the the power exponential relaxation is due to fast fluctuating magnetic fields. [24, 25] Thus, only the A_{SDW} signal appears below T_{SDW} , while the latter two signals are not affected by the formation of the IC-SDW order. Actually, the other parameters of the latter two signals, *i.e.*, λ_x , Δ and β_x , also seem to be independent of T . Hereby, we, therefore, ignore the contributions from these two signals.

The $V_{\text{F}}(T)$ curve increases monotonically with decreasing T below T_{SDW} , reaching a maximum at the lowest T is $V_{\text{F}}=50\%$ at 1.8 K. This value is significantly higher than in polycrystalline $\text{Na}_{0.75}\text{CoO}_2$ ($V_{\text{F}}=21\%$). [15] However, V_{F} for the c -aligned $[\text{Ca}_2\text{CoO}_3]_{0.62}^{\text{RS}}[\text{CoO}_2]$ and $[\text{Ca}_2\text{Co}_{4/3}\text{Cu}_{2/3}\text{O}_4]_{0.62}^{\text{RS}}[\text{CoO}_2]$ samples were found to be $\sim 100\%$. [18] Thus, the present $\text{Na}_{0.9}\text{CoO}_2$ crystals are considered to be still magnetically inhomogeneous, probably due to an inhomogeneous distribution of the Na ions. In particular, $\text{Na}_{0.9}\text{CoO}_2$ is reported to be unstable in humid air; [20] the excess Na easily reacts with moisture

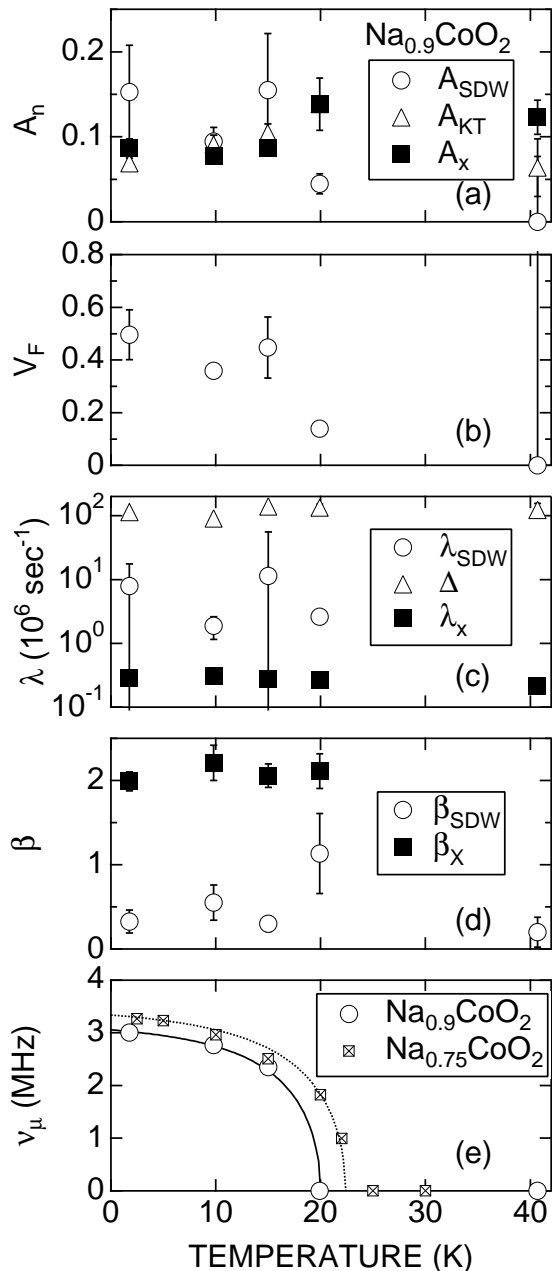


FIG. 5: Temperature dependences of (a) A_{SDW} , A_{KT} and A_x , (b) the volume fraction of the SDW signal (V_{F}), (c) λ_{SDW} , Δ and λ_x (d) β_{SDW} and β_x (e) ν_μ for the single crystal platelets of $\text{Na}_{0.9}\text{CoO}_2$. In Fig. 5(e), the $\nu_\mu(T)$ curve for the polycrystalline $\text{Na}_{0.75}\text{CoO}_2$ sample (ref. 14) is also shown, although its ZF- μ^+ SR spectrum was fitted by an exponentially damped cosine oscillation, $\exp(-\lambda t) \cos(\omega_\mu t + \phi)$. The solid and broken lines in Fig. 5(e) represent the temperature dependence of the BCS gap energy.

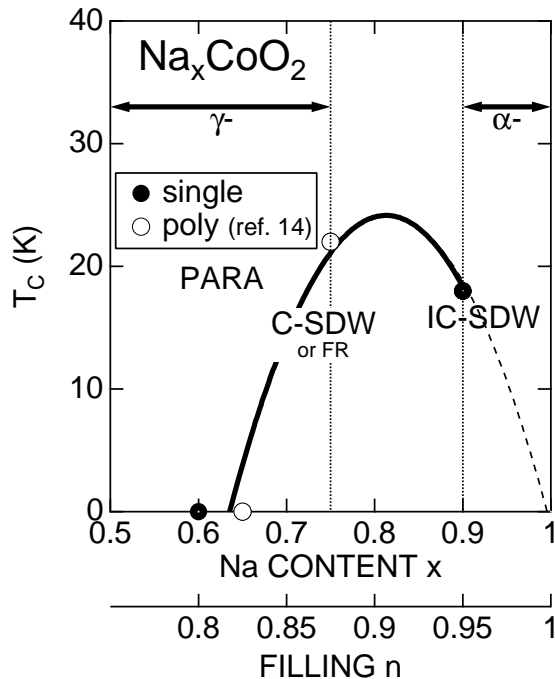


FIG. 6: Phase diagram of Na_xCoO_2 determined by μ^+ SR experiments. Solid circles represent the present result and open circles the previous data (ref. 14). The point at $x=1$ is a speculation from the data on the related compound LiCoO_2 . The relationship between structure and x is also shown; α and γ denote the α -phase and γ -phase. The β -phase ($0.55 \leq x \leq 0.6$) is unstable at high temperatures used for the sample preparation in the current work and changes to the γ -phase; hence, only the two (α and γ) phases are presented.

in air, although the present samples were kept in a desiccator prior to the μ^+ SR experiment. Both the temperature dependences of λ_{SDW} and β_{SDW} are fairly flat (see Figs. 5(c) and (d)), while, as T decreases, the ν_μ increases with a decreasing slope $d\nu_\mu/dT$ (Fig. 5(e)). This behavior is well explained by the BCS prediction for order parameter for the SDW state.[27] Since the value of $\nu_\mu(0 \text{ K})$ is estimated as 3.0 MHz, the internal magnetic field in the magnetically ordered state in $\text{Na}_{0.9}\text{CoO}_2$ is almost equivalent to that in the polycrystalline $\text{Na}_{0.75}\text{CoO}_2$ sample ($\nu_\mu(0 \text{ K}) \sim 3.3 \text{ MHz}$).[15]

IV. DISCUSSION

A. phase diagram and electron correlation

In the previous μ^+ SR experiment [15] on polycrystalline $\text{Na}_{0.75}\text{CoO}_2$ and $\text{Na}_{0.65}\text{CoO}_2$ samples, the Na-richer sample exhibited a transition to either a ferrimagnetic (FR) or a commensurate (C-) SDW state at 22 K,

whereas the Na-poorer sample was a paramagnet down to 2 K. Since the two samples were single phase of a hexagonal structure (γ -phase),[28] the magnetic transition at 22 K is considered to be an intrinsic behavior in $\text{Na}_{0.75}\text{CoO}_2$. Therefore, we can sketch the magnetic phase diagram of Na_xCoO_2 with $x \geq 0.6$ as a function of x (see Fig. 6). Recent compositional and chemical titration analyses indicated that the oxygen deficiency δ in $\text{Na}_x\text{CoO}_{2-\delta}$ is negligibly small even for the sample with $x=0.9$. [20] This means that the average Co valence is directly calculated from x . As x increases from 0.6 (*i.e.*, the Co valence decreases from 3.4), the magnitude of T_C increases up to a maximum at around $x=0.8$, decreases with further increasing x . As a result, we obtain a dome-shaped relationship between T_C and x for Na_xCoO_2 .

The crystal structure of $\text{Na}_{0.9}\text{CoO}_2$ (α -phase) is different from that of Na_xCoO_2 with $x \leq 0.75$ (γ -phase), as seen in Fig. 6. That is, in the α -phase, the sequence of the stacking of oxygen layers is represented as A-B-C-A-B-C, while in the γ phase A-B-B-A, where A, B, and C are named as similar for the stacking sequence in the face centered cubic close-packed structure. [12] Also, Na ions occupy the octahedral sites in the α -phase, while the prism sites in the γ phase. [12] It is worth noting that the μ^+ sites are bound to the O ions, indicating that the μ^+ mainly feel the magnetic field in the $[\text{CoO}_2]$ plane. Thus, the IC-SDW is most unlikely to be caused by the misfit between the two subsystems, but to be an intrinsic behavior of the $[\text{CoO}_2]$ plane.

The end member of Na_xCoO_2 , that is, a fully occupied Na_1CoO_2 phase can not be prepared by a conventional solid state reaction technique and/or a flux technique, [12, 20] while the related compound LiCoO_2 can be easily obtained. The structure of LiCoO_2 is isomorphous with $\alpha\text{-NaFeO}_2$ ($R\bar{3}m$) [29] and almost the same structure as that of the $\gamma\text{-Na}_x\text{CoO}_2$ phase, if we ignore the difference of the occupancy between the Na and the Li plane. LiCoO_2 is reported to be diamagnetic down to 4.2 K.[30] Since the Co^{3+} ions in LiCoO_2 are in a low-spin state t_{2g}^6 as in the case for Na_xCoO_2 , the diamagnetic behavior is expected. Therefore, NaCoO_2 is also speculated to lack magnetically ordered states.

The occupancy of Co^{4+} spins ($S=1/2$) on the two-dimensional triangular lattice 2DTL increases with decreasing x , so that the other end member, Na_0CoO_2 would have a half filled 2DTL. In other words, every lattice site is occupied by $S=1/2$. If we employ the Hubbard model within a mean field approximation as the basis for explaining the magnetism of such system; [31, 32, 33]

$$H = -t \sum_{\langle ij \rangle \sigma} c_{i\sigma}^\dagger c_{j\sigma} + U \sum_i n_{i\uparrow} n_{i\downarrow}, \quad (6)$$

where $c_{i\sigma}^\dagger$ ($c_{j\sigma}$) creates (destroys) an electron with spin σ on site i , $n_{i\sigma} = c_{i\sigma}^\dagger c_{i\sigma}$ is the number operator, t is the nearest-neighbor hopping amplitude and U is the Hubbard on-site repulsion. The electron filling n is defined

as $n = (1/2N)\sum_i^N n_i$, where N is the total number of sites.

At $T=0$ and $n=0.5$ (*i.e.*, Na_0CoO_2), as U increases from 0, the system is first a paramagnetic metal up to $U/t \sim 3.97$, then changes into a metal with a spiral IC-SDW, and then, at $U/t \sim 5.27$, a first-order metal-insulator transition occurs.[31] The lack of magnetic transitions for Na_xCoO_2 with $x=0.6$ and 0.65 suggests that $U/t \leq 3.97$. This means that Na_xCoO_2 is unlikely to be a strongly correlated electron system, because $U \gg t$ for such system. This conclusion is in good agreement with the magnitude of γ determined by the present C_p measurement ($\gamma=3.62\pm 0.04$ mJK⁻² per mol atom = 13.03 ± 0.14 mJK⁻² per mol Co for $\text{Na}_{0.6}\text{CoO}_2$). This value is 18.5 times larger than that of Cu.

Also the calculations predict that, [32, 33] as n increases from 0, the magnitude of U/t at the boundary between the paramagnetic and SDW phases decreases with increasing slope ($d(U/t)/dn$) up to $n=0.75$. Even for $U/t=0$, the SDW phase is stable at $n=0.75$. U/t increases with further increasing n , with decreasing slope. Therefore, the dome-shaped relationship found in the phase diagram (Fig. 6) is qualitatively explained by the model calculations, although the maximum located at around $x=0.8$ (*i.e.* $n=0.9$). Furthermore, it is most likely that $\text{Na}_{0.75}\text{CoO}_2$ enters the C-SDW state below 22 K rather than the ferrimagnetic state, because the magnetism in Na_xCoO_2 seems to be totally understood by Eq. (6).

B. magnitude of internal magnetic field

If the SDW state is induced by the competition between U/t and n in the CoO_2 2DTL, the nature of the SDW state is considered to be essentially same in all the cobaltites. However, the internal magnetic field of the ordered state, $\nu_\mu(0$ K), is found to be ~ 3 MHz for Na_xCoO_2 , while it is ~ 60 MHz for $[\text{Ca}_2\text{CoO}_3]_{0.62}^{\text{RS}}[\text{CoO}_2]$ and $[\text{Ca}_2\text{Co}_{4/3}\text{Cu}_{2/3}\text{O}_4]_{0.62}^{\text{RS}}[\text{CoO}_2]$. [16, 18] The muon locates probably ~ 0.1 nm away from the oxygen ions, and there is no space for it in the CoO_6 octahedra in the $[\text{CoO}_2]$ plane as in the case for the high- T_c cuprates[25]. This discrepancy is difficult to explain only by differences in the μ^+ site experiencing the SDW field. That is, even if the μ^+ s in Na_xCoO_2 locate in the vacant sites in the Na plane and those in the latter two cobaltites are bound to oxygen in the CoO_2 plane, the ratio between the bond length d of Na-Co and O-Co is about 1.65. Assuming that $\nu_\mu(0$ K)=60 MHz at the oxygen site in the CoO_2 plane, $\nu_\mu(0$ K) at the Na site would be roughly ~ 13 MHz, because the dipolar field is proportional to d^{-3} . This is still four times larger than the experimental result.

Hence, there should be the other reasons for the lower $\nu_\mu(0$ K) found in Na_xCoO_2 . Considering the crystal structure of these cobaltites, the distance between adjacent CoO_2 planes in Na_xCoO_2 is signifi-

cantly smaller than those in $[\text{Ca}_2\text{CoO}_3]_{0.62}^{\text{RS}}[\text{CoO}_2]$ and $[\text{Ca}_2\text{Co}_{4/3}\text{Cu}_{2/3}\text{O}_4]_{0.62}^{\text{RS}}[\text{CoO}_2]$. Thus, the interlayer interaction between the CoO_2 planes in Na_xCoO_2 is considerably larger than in the other layered cobaltites. Such interaction is thought to weaken the two dimensionality of the CoO_2 plane. As a result, the magnitude of $\nu_\mu(0$ K) in Na_xCoO_2 may be smaller than those in the other layered cobaltites. Indeed, large transition widths, $\Delta T \sim 70$ K, were observed in $[\text{Ca}_2\text{CoO}_3]_{0.62}^{\text{RS}}[\text{CoO}_2]$ and $[\text{Ca}_2\text{Co}_{4/3}\text{Cu}_{2/3}\text{O}_4]_{0.62}^{\text{RS}}[\text{CoO}_2]$, while $\Delta T \sim 0$ K for Na_xCoO_2 . This suggests an increase in spin frustration, reflecting the decrease in the two-dimensionality in Na_xCoO_2 .

V. SUMMARY

In order to elucidate the magnetism in 'good' thermoelectric layered cobaltites, μ^+ SR spectroscopy and heat capacity (C_p) measurements were performed on single crystals of Na_xCoO_2 with $x = 0.6$ and 0.9 in the temperature range between 250 and 1.8 K.

Both χ_c , C_p and weak-transverse-field (wTF-) μ^+ SR measurements on $\text{Na}_{0.9}\text{CoO}_2$ indicated the existence of a magnetic transition at 19 K, although no transitions were detected in $\text{Na}_{0.6}\text{CoO}_2$ down to 1.9 K. A clear oscillation in the zero-field (ZF-) μ^+ SR spectra, fitted by a Bessel function, suggested that $\text{Na}_{0.9}\text{CoO}_2$ enters an incommensurate spin density wave state below 19 K ($=T_{5\text{DW}}$). In addition, the IC-SDW was found to propagate in the c plane (*i.e.*, the CoO_2 plane), with oscillating moments directed along the c -axis, similar to $[\text{Ca}_2\text{CoO}_3]_{0.62}^{\text{RS}}[\text{CoO}_2]$.

By reference to the previous μ^+ SR results on polycrystalline samples, a tentative magnetic phase diagram was obtained for Na_xCoO_2 with $x \geq 0.6$. The relationship between $T_{5\text{DW}}$ and x changed dome-shaped, as well as the change in the high- T_c cuprates. Since this relationship was explained using the Hubbard model within a mean field approximation for two-dimensional triangle lattice of the CoO_2 plane, which is a common structural component for the all known thermoelectric layered cobaltites, this bell-shape relationship is concluded to be a common behavior for the layered cobaltites.

The absence of the SDW state in $\text{Na}_{0.6}\text{CoO}_2$ provided the upper limit for the magnitude of U/t as 3.97, where U denotes the Hubbard on-site repulsion and t the nearest-neighbor hopping amplitude. This indicated that $\text{Na}_{0.6}\text{CoO}_2$ is a moderately correlated electron system, although it is believed to be a strongly correlated system. This conclusion was consistent with the measured electronic specific heat parameter (γ) of $\text{Na}_{0.6}\text{CoO}_2$, because γ was almost equivalent to the calculated value without an electron correlation.

Acknowledgments

We thank Dr. S.R. Kreitzman and Dr. D.J. Arseneau of TRIUMF for help with the μ^+ SR experiments. Also, we thank Dr. Y. Seno and Dr. C. Xia of Toyota CRDL, Mr. A. Izadi-Najafabadi and Mr. S.D. LaRoy of University of British Columbia for help with the experiments. We appreciate useful discussions with Dr. T. Tani and

Dr. R. Asahi of Toyota CRDL, Professor U. Mizutani, Professor H. Ikuta and Professor T. Takeuchi of Nagoya University and Professor K. Machida of Okayama University. This work was supported at UBC by the Canadian Institute for Advanced Research, the Natural Sciences and Engineering Research Council of Canada, and at TRIUMF by the National Research Council of Canada.

-
- [1] J. Molenda, C. Delmas, P. Dordor, and A. Stoklosa, *Solid State Ionics*, **12**, 473 (1989).
- [2] H. Yakabe, K. Kikuchi, I. Terasaki, Y. Sasago, K. Uchinokura, in *Proceedings of 16th International Conference on Thermoelectrics*, Dresden, 1997 (Institute of Electrical and Electronics Engineers, Piscataway, 1997), pp.523-527.
- [3] I. Terasaki, Y. Sasago, and K. Uchinokura, *Phys. Rev. B* **56**, R12685 (1997).
- [4] R. Funahashi, I. Matsubara, H. Ikuta, T. Takeuchi, U. Mizutani, and S. Sodeoka, *Jpn. J. Appl. Phys.* **39**, L1127 (2000).
- [5] A. C. Masset, C. Michel, A. Maignan, M. Hervieu, O. Toulemonde, F. Studer, B. Raveau, and J. Hejtmanek, *Phys. Rev. B* **62**, 166 (2000).
- [6] Y. Miyazaki, K. Kudo, M. Akoshima, Y. Ono, Y. Koike and T. Kajitani, *Jpn. J. Appl. Phys.* **39**, L531 (2000).
- [7] I. Tsukada, T. Yamamoto, M. Takagi, T. Tsubone, S. Konno, and K. Uchinokura, *J. Phys. Soc. Jpn.* **70**, 834 (2001).
- [8] Y. Miyazaki, T. Miura, Y. Ono, and T. Kajitani, *Jpn. J. Appl. Phys.* **41**, L849 (2002).
- [9] K. Takada, H. Sakurai, E. Takayama-Muromachi, F. Izumi, R. A. Dilanian, and T. Sasaki, *Nature* **422**, 53 (2003).
- [10] R. E. Schaak, T. Klimczuk, M. L. Foo, R. J. Cava, *Nature* **424**, 527 (2003).
- [11] Y. Wang, N. S. Rogado, R. J. Cava, N. P. Ong, *Nature* **423**, 425 (2003).
- [12] C. Fouassier, G. Matejka, J-M. Reau, and P. Hagenmuller, *J. Solid State Chem.*, **6**, 532 (1973).
- [13] Von M. Jansen, and R. Hoppe, *Z. Anorg. Allg. Chem.*, **408**, 104 (1974).
- [14] T. Motohashi, R. Ueda, E. Naujalis, T. Tojo, I. Terasaki, T. Atake, M. Karppinen, and H. Yamauchi, *Phys. Rev. B* **67**, 64406 (2003).
- [15] J. Sugiyama, H. Itahara, J. H. Brewer, E. J. Ansaldo, T. Motohashi, M. Karppinen, and H. Yamauchi, *Phys. Rev. B* **67**, 214420 (2003).
- [16] J. Sugiyama, H. Itahara, T. Tani, J. H. Brewer, and E. J. Ansaldo, *Phys. Rev. B* **66**, 134413 (2002).
- [17] J. Sugiyama, C. Xia, and T. Tani, *Phys. Rev. B* **67**, 104410 (2003).
- [18] J. Sugiyama, J. H. Brewer, E. J. Ansaldo, H. Itahara, K. Dohmae, Y. Seno, C. Xia, and T. Tani, *Phys. Rev. B* **68**, 134423 (2003).
- [19] M. Mikami, M. Yoshimura, Y. Mori, T. Sasaki, R. Funahashi and M. Shikano, in *Proceedings of 21st International Conference on Thermoelectrics*, Long Beach, 2002 (Institute of Electrical and Electronics Engineers, Piscataway, 2002), pp.223-225.
- [20] M. Mikami, M. Yoshimura, Y. Mori, T. Sasaki, R. Funahashi, and M. Shikano, *Jpn. J. Appl. Phys.* (in press).
- [21] L. P. Le, A. Keren, G. M. Luke, B. J. Sternlieb, W. D. Wu, Y. J. Uemura, J. H. Brewer, T. M. Riseman, R. V. Upasani, L. Y. Chiang, W. Kang, P. M. Chaikin, T. Csiba, and G. Grüner, *Phys. Rev. B* **48**, 7284 (1993).
- [22] Y. Ando, N. Miyamoto, K. Segawa, T. Kawata, and I. Terasaki, *Phys. Rev. B* **60**, 10580 (1999).
- [23] D. J. Singh, *Phys. Rev. B* **61**, 13397 (2000).
- [24] Y. J. Uemura, in *Muon Science* edited by S. L. Lee *et al.*, (Institute of Physics Publishing, Bristol, 1999) pp. 85-114, and references cited therein.
- [25] G. M. Kalvius, D. R. Noakes, and O. Hartmann, in *Handbook on the Physics and Chemistry of Rare Earths* **32** edited by K. A. Gschneidner Jr. *et al.*, (North-Holland, Amsterdam, 2001) pp. 55-451, and references cited therein.
- [26] K. M. Kojima, Y. Fudamoto, M. Larkin, G. M. Luke, J. Merrin, B. Nachumi, Y. J. Uemura, M. Hase, Y. Sasago, K. Uchinokura, Y. Ajiro, A. Revcolevschi, and J. -P. Renard, *Phys. Rev. Lett.* **79**, 503 (1997).
- [27] G. Grüner; *Density Waves in Solids* Chap. 4 (Addison-Wesley-Longmans, Reading, 1994), and references cited therein.
- [28] T. Motohashi, E. Naujalis, R. Ueda, K. Isawa, M. Karppinen, and H. Yamauchi, *Appl. Phys. Lett.* **79**, 1480 (2001).
- [29] T. A. Hewston and B. Chamberland, *J. Phys. Chem. Solids* **48**, 97 (1987) and references cited therein.
- [30] I. Tomeno and M. Oguchi, *J. Phys. Soc. Jpn* **67**, 318 (1998).
- [31] H. R. Krishnamurthy, C. Jayaprakash, S. Sarker, and W. Wenzel, *Phys. Rev. Lett.* **64**, 950 (1990).
- [32] M. Fujita, M. Ichimura, and K. Nakao, *J. Phys. Soc. Jpn.* **60**, 2831 (1991).
- [33] M. Fujita, T. Nakanishi, and K. Machida, *Phys. Rev. B* **45**, 2190 (1992).